Geo-Routing Algorithms and Protocols for Power Line Communications in Smart Grids

Mauro Biagi, *IEEE Senior Member*, Simone Greco and Lutz Lampe, *IEEE Senior Member*

***Abstract*—Making electric power grids smart is invariably linked to the implementation of an advanced communication infrastructure that is able to transport sensing, control and automation information timely, reliably and efficiently. Reusing the power line themselves to realize (part of) this infrastructure is an obvious choice that has a long and successful track record with power utilities. In this paper, we propose to make use of the fact that the nodes of a power line communications (PLC) network are stationary to deliver messages fast and energy efficiently through routes consisting of a series of communication links. In particular, we exploit location information of PLC nodes to route a message along a favorable path. Such geographic or geo-routing is particularly apt for PLC networks with time-varying link qualities, where optimal routes will change with time. We present routing algorithms and protocols for unicast, broadcast and multicast transmission that use network topology knowledge to determine the message path taking energy and delay constraints into account. We focus on the distribution domain of the power grid and propose decentralized solutions that use of information about the communication neighborhood of a node, which is acquired through proper signaling in the grid.**

***Index Terms*—Power line communications (PLC), Geographic Routing, Smart Grid, Protocols**

I. Introduction

Efficient and reliable communication is a pre-requisite for the vision of smart electricity grids to come true. One natural choice for the medium of communication are the electrical power lines themselves. This power line communication (PLC) has a long history and a proven track record for enabling telemetry, control and automation in the electric power grid [3], [4], [5]. In many scenarios, the communication from a data source to its destination is accomplished via multiple transmissions using intermediate communication nodes. In this case, since the power line medium realizes a broadcast channel with generally not well defined boundaries for signal propagation, the question of finding the best path or route for the transmission of a message arises. Further, since the link quality of a PLC channel is generally time varying, the best route may change over time. There is extensive literature addressing the problem of routing for smart grids, see for example the survey papers [6], [7], [8]. In the context of PLC for smart grids, the Lightweight On-demand Ad hoc Distance-vector routing protocol (LOAD) and LOAD-Next Generation (LOADng) and the Routing Protocol for Low power and lossy networks (RPL) have been studied [9], [10], [11]. The former is a reactive protocol that establishes a route on demand, while RPL establishes routes proactively. Both protocols determine the route before transmission of the data packets.

In this work, we consider an instance of opportunistic routing, in which the route is established at the point of transmission to take full advantage of the broadcast nature of the medium. An example of such an approach is the flooding-type routing using single-frequency network (SFN) transmission discussed for PLC in [12]. While SFN-based flooding requires very little routing overhead and quickly adapts to changes in network connectivity, it suffers from high resource occupation and low energy efficiency. To avoid the waste of transmission opportunities and energy associated with flooding, in [1], [2] we have introduced the concept of routing using location information of network nodes, i.e., geo-routing, for PLC. Location-based routing is known from wireless communications [13] and routing algorithms include Beacon Less Routing (BLR) [14], Implicit Geographic Forwarding (IGF) [15] and Beacon Based Routing (BBR) [16]. The basic rationale for geo-routing for PLC is that communications nodes are invariably immobile. Hence, while link quality is generally varying, the underlying grid topology and thus locations of PLC nodes are completely static. This has also been recently used in [17], where a Request to Send / Clear to Send (RTS/CTS) mechanism is used jointly with an opportunistic method for forwarding information aimed at reducing interference and efficiently using the medium. Packet delivery time (latency) and energy spent for transmission have not been analyzed though.

In this paper, we first revisit the problem of unicast geo-routing first suggested in [1], [2]. We introduce the effect of network traffic and thus queuing delay into the problem formulation and also allow for adjustment of the transmission rate to the link quality, which not only affects transmission delay but also the energy spent for the transmission of a message. Thus, our main objectives are to minimize the transmission energy and delay required for routing a message through a PLC network. Furthermore, we extend the problem to the transmission of broadcast and multicast messages. In the proposed methods, we make use of topology knowledge and achieve reliability of transmission through opportunistically selecting forwarding nodes. To this end, we present a packet structure for the necessary local information exchange and a protocol for implementing the geo-routing considering the

Mauro Biagi and Simone Greco are with DIET, University of Rome Sapienza, Rome, Italy. Lutz Lampe is with the Dept. of Electr. and Comp. Eng., University of British Columbia, Vancouver, Canada. Parts of this work have been presented at the IEEE International Conference on Smart Grid Communications (SmartGridComm) 2010 [1] and the IEEE International Symposium on Power Line Communications (ISPLC) 2012 [2]. This work has been supported in part by the Natural Sciences and Engineering Research Council of Canada (NSERC).

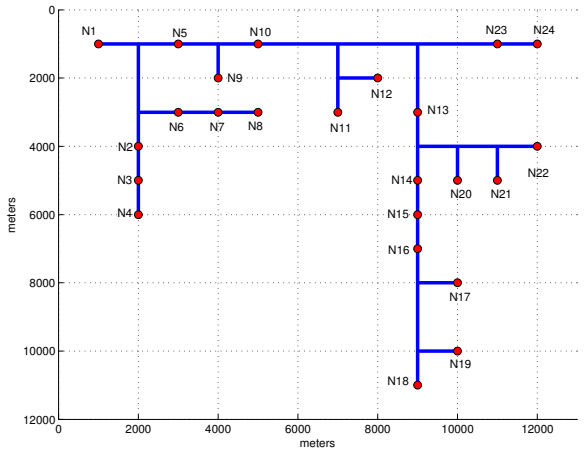

Fig. 1. An example for a part of a power distribution network with PLC nodes N1 to N24.

effect of network traffic and queuing in each PLC node. To highlight the effectiveness of our proposal, numerical performance evaluations and comparisons with alternative algorithms are presented.

The proposed geo-routing is a decentralized method based on the concept of nodes having knowledge about their neighborhood. Related work in the domain of wireless communication is the Local Broadcast Algorithm (LBA) proposed in [18]. In that work the goal is to minimize the number of transmissions by all nodes under the implicit assumption of perfect local knowledge of the channel parameters. However, energy consumption has not been considered, as minimizing the number of transmissions minimizes delay but does not explicitly account for energy consumption. Broadcast geo-routing has been discussed in [19] using a centralized approach though, and the solution in [20] makes use of the existing query routing tree to reduce the number of retransmissions. Multicast geo-routing has been studied in the context of sensor or mobile ad hoc networks in [21], [22], [23], [24], [25]. These works consider the packet delivery time and/or the delivery ratio, i.e., the percentage of reached destinations. To do so greedy solutions to graph theoretical approaches have been considered, but network dynamics (link quality changes) and/or queuing at the relay nodes have not been included.

The remainder of the paper is organized as follows. The PLC network model and the routing objective are presented in Section II. In Section III, we describe the proposed decentralized routing algorithms, which are embedded into a protocol in Section IV. Numerical results are presented and discussed in Section V. Conclusions are provided in Section VI.

II. Network Description and Cost Function

Figure 1 illustrates an example PLC network located in part of a medium voltage / low voltage (MV/LV) distribution grid considered in this work. While the physical location of nodes and the physical connections through power lines are static, the logical connectivity between nodes is dynamic. This is due to the dynamics of power loads (e.g., changing impedance, switching of loads), which lead to changes in the node-to-node channel transfer functions, changes in the noise ingress onto power lines and thus noise experienced at nodes, and node sleep cycles (nodes turning off and on). Hence, while the network topology is static, network connectivity is time-variant. These characteristics motivate the development of routing algorithms able to react to network changes and using location information. Before introducing the routing algorithms, a formal definition of the network must be provided, for which we chose a graph model which includes bus, tree, and ring structures as experienced in distribution grids.

A. Network Model

We describe the PLC network as the graph

$$\mathcal{G} = \{\mathcal{N}, \mathcal{E}\} \tag{1}$$

consisting of the set

$$\mathcal{N} = \{1, ..., N\} \tag{2}$$

of N vertexes, representing network nodes (i.e., PLC modems), and the edge set

$$\mathcal{E} = \{(i,j) : M_{ij} \geq Q\} \ , \tag{3}$$

representing network connections over power lines. According to (3), nodes i and j are connected if the quality metric M_{ij} for this link exceeds a minimal required value Q. Hence, the (one-hop) neighborhood for a node $i \in \mathcal{N}$ is defined as

$$\mathcal{R}_i = \{j \in \mathcal{N} | (i,j) \in \mathcal{E}\} \ . \tag{4}$$

As in [1], [2], we base the quality metric on the achievable rate, which for the link between nodes i and j is given by

$$C_{ij}(P_{ij}) = \int_{B_1}^{B_2} \log_2 \left(1 + \frac{P_{ij}|H_{ij}(f)|^2}{(B_2 - B_1)N(f)\Gamma}\right) \mathrm{d}f \ . \tag{5}$$

P_{ij} is the transmit power used by node i for transmitting to node j, $N(f)$ is the noise power spectral density (PSD), $H_{ij}(f)$ is the frequency response of the PLC channel between nodes i and j, B_1 and B_2 are the lower and upper frequency of the band, and Γ accounts for signal-to-noise (SNR) gap between channel capacity and achievable rate using practical coding and modulation schemes. Note that we assume that the PLC signal is transmitted with a frequency-flat PSD of $P_{ij}/(B_2 - B_1)$. The link quality metric M_{ij} is then obtained as

$$M_{ij} = C_{ij}(P_{\max}) \ , \tag{6}$$

where $P_{\max}$ is the maximal permitted transmit power.

B. Cost Function

Given a graph model of the network, routes are generally established based on the evaluation of cost function associated with a path. In this work, we apply a cost function U that captures latency and energy consumption for the delivery of a message. If a message of W bits is to be transmitted from node i to node j, then the required transmit energy is given

by $E_{ij} = P_{ij}T_{ij}$, where $T_{ij} = W/C_{ij}(P_{ij})$ is the associated transmission delay. Furthermore, the delay parameter $\tau_{ij} = T_{ij} + q_j$ accounts for the transmission delay T_{ij} and the expected queuing delay q_j at the node j, which depends on the traffic level in the PLC network.

Denoting the set containing all the ordered sequences of single hops, corresponding to pairs of nodes that can be used for connecting a source node S with a destination node D as $\mathcal{P}(S,D)$, and its elements by π_m, $m = 1, 2, \ldots, |\mathcal{P}|$, the cost function associated with the mth path π_m is defined as

$$U_{\pi_m} = \sum_{(i,j)\in\pi_m} a_T \tau_{i,j} + a_E E_{i,j} \ , \tag{7}$$

where a_T (with unit sec^{-1}) and a_P (with unit Joule^{-1}) are the weights to trade-off the two objectives.

C. Centralized Route Optimization

As a starting point for decentralized geo-routing methods presented in the next section, let us consider the formulation of a centralized routing optimization, which requires a node (e.g., the source) having a full knowledge about link qualities in the network. Acquiring this knowledge can be very costly in terms of communication overhead and it is prone to become stale due to link variations. Considering the cost function (7), the unicast route optimization problem can be written as

$$\min_{\pi_m\in\mathcal{P}(S,D)} U_{\pi_m}, \tag{8a}$$

$$\text{s.t.} \quad \sum_{(i,j)\in\pi_m} E_{i,j} \le E_{\max} \tag{8b}$$

$$\sum_{(i,j)\in\pi_m} \tau_{i,j} \le \tau_{\max}, \tag{8c}$$

where the first constraint puts a cap on the maximum energy that can be spent for message delivery and the second constraint limits the message latency. The above expression considers a single destination node D and will be the starting point to solve the unicast routing problem in a decentralized way. We then extend this approach to present decentralized routing for multicast and broadcast transmission.

III. Neighborhood-Knowledge Based Decentralized Geo-routing

For solving (a version of) (8) in a decentralized fashion, we assume that a node i has pertinent information from nodes within its $K^\star$-hop neighborhood. $K^\star = 1$ means that a node receives status information only from its direct neighbors, $K^\star = 2$ includes neighbors' neighbors, and so forth. This information is shared by periodically sending cumulative hello messages (C-hms). These C-hms have variable length depending on the neighborhoods' compositions. The set $\mathfrak{N}_i(K)$ of nodes in the K-hop neighborhood of node i is given by the recursion

$$\begin{aligned} \mathfrak{N}_i(1) &= \mathcal{R}_i, \\ \mathfrak{N}_i(K) &= \mathfrak{N}_i(K-1) \cup_{j\in\mathfrak{N}_i(K-1)} \mathcal{R}_j \ . \end{aligned} \tag{9}$$

A. Unicast Geo-routing

We first consider unicast routing. For this, let us assume that a node i is the ℓ-th relay on the route of a packet. In our decentralized routing approach, node i selects the $(\ell+1)$-st relay based on its knowledge about its neighborhood $\mathfrak{N}_i(K^\star)$ and the location information of nodes in the network. The neighborhood knowledge allows node i to look L_i hops ahead, where the value of L_i depends on the investigated route. For the following, let us denote the set of routes from node i via nodes $j \in \mathfrak{N}_i(K^\star)$ by $\mathcal{P}(i, K^\star)$ and its elements by π_m, $m = 1, 2, \ldots, |\mathcal{P}(i, K^\star)|$. The last node of the route π_m is $f(m)$. Furthermore, we denote the total energy and time consumed along the route from the source node to node i by $\bar{E}_i$ and $\bar{\tau}_i$, respectively. Then, we propose to select the $(\ell+1)$-st relay by solving the following minimization problem:

$$\min_{\pi_m\in\mathcal{P}(i,K^\star)} \quad U_{\pi_m} G(\bar{\tau}_i, \pi_m) Z(\bar{E}_i, \pi_m) \Delta_{f(m)} \tag{10a}$$

$$\text{s.t.} \quad \bar{E}_i + \sum_{(j,k)\in\pi_m} E_{j,k} \le E_{\max}, \tag{10b}$$

$$\bar{\tau}_i + \sum_{(j,k)\in\pi_m} \tau_{j,k} \le \tau_{\max}. \tag{10c}$$

In the centralized framework (8) the utility U_{π_m} sufficed to solve the constrained routing problem. Since for the distributed approach the neighborhood knowledge does not cover the whole network, we need to introduce three auxiliary functions that are $G(\bar{\tau}_i, \pi_m)$, $Z(\bar{E}_i, \pi_m)$ and $\Delta_{f(m)}$ to avoid eventually failing the constraints.

The function G is defined as

$$G(\bar{\tau}_i, \pi_m) = \left(1 - \frac{\bar{\tau}_i + \sum\limits_{(j,k)\in\pi_m} \tau_{j,k}}{\tau_{\max}}\right)^{-\alpha} , \tag{11}$$

and it tries to penalize routes that, if choosing a relay, may cause violation of constraint (10c). This aspect becomes important when the delay $\bar{\tau}_i$ is approaching $\tau_{\max}$. The exponent $\alpha > 0$ shapes the penalty function, with larger α putting more emphasis on the delay constraint. Similarly, we define

$$Z(\bar{E}_i, \pi_m) = \left(1 - \frac{\bar{E}_i + \sum\limits_{(j,k)\in\pi_m} E_{j,k}}{E_{\max}}\right)^{-\eta} , \tag{12}$$

with parameter $\eta > 0$, to discourage the choice of relays that may lead to violating the energy constraint (10b). Finally, in order to choose the right *direction* toward the destination, we consider the function

$$\Delta_{f(m)} = (1 + \rho d_{f(m),D})^{\beta} \tag{13}$$

that evaluates how close the destination can be reached by a considered route. It includes location information in the routing selection through the physical distance $d_{f(m),D}$ between nodes $f(m)$ and D. The parameter ρ (meter^{-1}) is used to normalize distances, while $\beta > 0$ gives emphasis to the distance term with respect to the others two auxiliary functions.

Practically speaking, when the source node $S = k(1)$ wants to send packets to the destination node D, depending

on the neighborhood knowledge that the source node has, it evaluates the next possible relay. This is done not only by considering the behavior of the network within the source node's neighborhood, but also by considering the network topology to assess possible future hops. Once the next relay has been selected, the source sends the packet, which contains the address of the next selected relay. The next relay proceeds in the same manner until the packet reaches the destination. The level of neighborhood knowledge determines how far a node can look ahead to make the choice for the next relay. The geo-information is explicitly accounted by $\Delta_{f(m)}$, since it helps to avoid to follow a route leading the packet away from its destination.

However, since the selection of the next relay node only solves a local optimization problem, a consequence of the decentralized nature of routing is that a violation of the delay and energy bounds in future steps may be unavoidable, i.e., (10) may become unfeasible and as a result a packet is dropped. This possibility of a packet loss is counteracted by functions (11) and (12), which penalize high-energy and high-delay partial paths respectively. The event that a packet is dropped implicitly means that some energy has been spent in vain as a result of the limited neighborhood knowledge. Hence, it is important to set the bounds to achieve a favorable trade-off between forcing low-energy paths and unwanted packet loss.

Furthermore, when the packet is forwarded by a relay, the previous relay is able to overhear the packet transmission, and this works as an implicit acknowledgement (ACK) as also used for BLR and BBR [1]. Since no retransmission occurs if the destination has been reached, only in this case an explicit ACK is sent by the destination to inform the last relay.

The larger the neighborhood knowledge and thus $K^\star$, the longer the C-hms packets become, since they must contain information about more neighborhoods. Hence, energy spent for signalling may not be negligible compared to that used for data transmission. We note that neighborhood size is not a function of the size of the network, but rather node density, which is governed by the physical density of nodes and the rate requirements to establish reliable links. Thus, while decentralized routing and signaling via C-hms is scalable with network size, a mechanism for turning off nodes can be useful for areas with high node density. More details about C-hms will be provided in Section IV.

B. Broadcast and Multicast Geo-routing

Broadcast and multicast cannot be described exactly by the formulation in (10) since multiple destinations, denoted by the set $\mathcal{D} \subset \mathcal{N}$, are present. Differently from geo-routing for unicast where only topology knowledge and neighborhood composition are needed, here also the information about nodes already reached by the broadcast or multicast message must be taken into account. In the following, we explain the necessary modifications to the routing method for unicast transmission.

First, similar to unicast transmission, we aim at progressing fast through the network in a cost-efficient manner. To this end, the node D^* of $\mathcal{D}$ that has not been reached yet by routing and is furthest away from a selected relay node is chosen as the destination and used in $\Delta_{f(m)}$. In doing so, we establish a route, which we refer to as *main flow*, along which a number of nodes are reached. If we denote the ℓth relay along the main flow as $k(\ell)$ and the set of yet unreached nodes after the ℓth hop as $\mathfrak{U}_{k(\ell)} \subseteq \mathcal{D}$, we have $D^* = \text{argmax}_{D \in \mathfrak{U}_{k(\ell)}} d_{k(\ell),D}$.

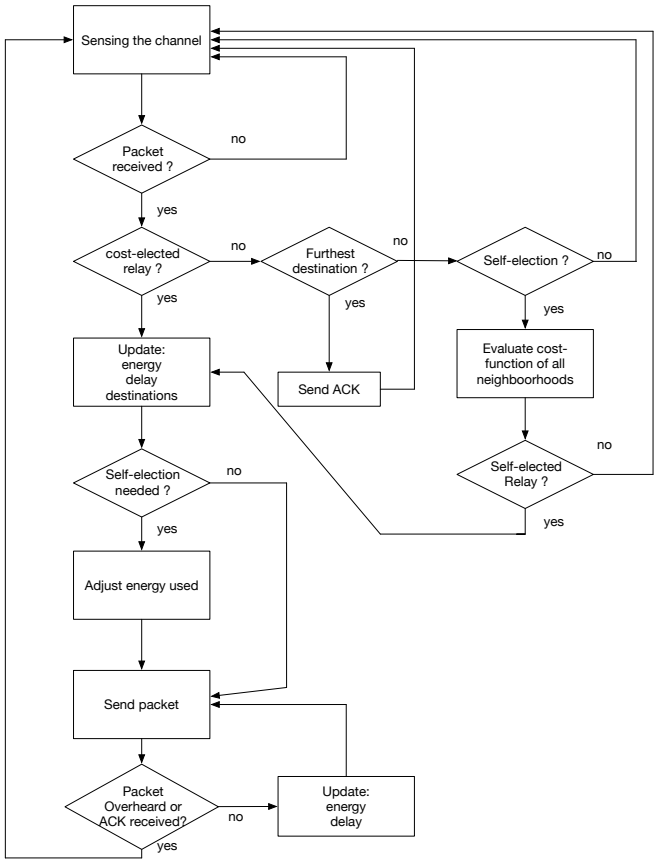

Fig. 2. Flowchart of routing at a network node.

The relays along the main flow are referred to as *cost-elected* relays. Since not all target nodes may be reached through the main flow, an additional relay selection mechanism needs to be realized. We refer to this additional mechanism as *self-election*. While cost-elected relays have been chosen by the preceding relay based on cost arguments, in the second mechanism a node elects itself when it understands that the packet cannot reach its neighbors. This may happen since the routing procedure follows the main flow and the neighbors of the (possible upcoming) self-elected relay do not belong to the main flow. The self-election is still made on the basis of the cost function.

Figure 2 shows the flowchart of the routing procedure at a network node. At the beginning of transmission (multicast or broadcast) the source $S \equiv k(1)$ selects the next relay (cost-elected) $k(2)$ on the basis of the most-distant destination and updates the list of the still-not achieved destinations that, in this case, are all the destinations with the exception of source neighborhood: $\mathfrak{U}_{k(1)} = \mathcal{D} \setminus \mathcal{R}_{k(1)}$.

When a packet has been received by a selected relay $k(\ell)$, it selects the next relay as specified above and updates the

energy used $\overline{E}_{k(\ell)}$ by considering the energy to be spent to achieve the next relay, the delay $\overline{\tau}_{k(\ell)}$ by considering also the queue time and transmission delay, and the not yet reached destinations according to the rule $\mathfrak{U}_{k(\ell)} = \mathfrak{U}_{k(\ell-1)} \setminus \mathcal{R}_{k(\ell)}$.

Before forwarding the packet, the current relay $k(\ell)$ considers based on topology knowledge, the previous relay $k(\ell-1)$ and the selected relay $k(\ell+1)$ and their neighborhoods, whether some destinations will be not be reached through future hops of the main flow. The nodes that cannot be reached by the main flow at relay $k(\ell)$ are collected in the set $\mathfrak{W}_{k(\ell)}$. If it is not empty, the relay understands that a self-election will take place, which implies that some energy will be used for forwarding the packet not on the main flow. The current relay thus increments the consumed energy $\overline{E}_{k(\ell)}$ by a margin E_{M} that accounts for how many nodes should be reached with self-election. The margin is set to $E_{\mathrm{M}} = \xi E_{\mathrm{peak}}$, where E_{peak} is the maximum energy that a node could use to transmit a packet over a reliable link. The value of ξ is an estimation of the minimum number of neighborhoods covering the nodes to be reached through self-election. If this margin is estimated too large, it reduces the remaining energy on the main flow, which may lead to unnecessary packet drops. Furthermore, the set of destinations is updated by the current relay according to the rule $\mathfrak{U}_{k(\ell)} = \mathfrak{U}_{k(\ell-1)} \setminus (\mathcal{R}_{k(\ell)} \cup \mathfrak{W}_{k(\ell)})$. This updated set is passed to the next cost-elected relay $k(\ell+1)$. On the other hand, if self-election is not needed, the current relay simply forwards the packet and waits for implicit ACK as specified before in unicast routing. If relay $k(\ell)$ is unable to overhear a forwarding message, it resends the packet. In case the current relay is able to reach all the remaining destinations, an explicit ACK is sent by the furthest destination.

If a node that received a packet is not the selected relay, it needs to determine whether a self-election is needed. This is illustrated in the right part of the flowchart in Figure 2. To this end, it determines the set $\mathfrak{W}_{k(\ell)} = \mathfrak{U}_{k(\ell-1)} \setminus (\mathfrak{U}_{k(\ell)} \cup \mathcal{R}_{k(\ell)})$. Knowledge of $\mathfrak{U}_{k(\ell-1)}$ is available at nodes which are both in $\mathcal{R}_{k(\ell-1)}$ and $\mathcal{R}_{k(\ell)}$. If there is not a node that belongs to both neighborhoods, the self-election does not start and a packet loss is experienced. If the set $\mathfrak{W}_{k(\ell)}$ is not empty, a self-election is needed. Then, the node evaluates cost function (10) for itself and its neighbors that also received both $\mathfrak{U}_{k(\ell-1)}$ and $\mathfrak{U}_{k(\ell)}$, so as to reach the furthest destination in $\mathfrak{W}_{k(\ell)}$. If the current node is the one with the lowest cost, it becomes the self-elected relay and, from there, an additional main flow starts until all nodes in $\mathfrak{W}_{k(\ell)}$ have been reached. That is, the node operates exactly as a cost-elected relay from there on. In principle, multiple cascaded self-elections are possible, leading to multiple active flows in the network.

To briefly illustrate the propagation and generation of flows, consider the network in Figure 1 and assume node N1 is the source node that broadcasts a message. In a typical scenario (more details are provided in the results section) node N10 will be selected as the next relay, which then selects node N12. The message from N1 also reaches nodes N2, N5, N6 and N9, but not N3, N4, N7, N8, which are also not reachable by N10. Hence, a self-election occurs on the vertical branch. Based on this, there are three scenarios: N2 becomes self-elected node (which means N2 must be able to reach at least N7 or N8), N6 becomes self-elected node (which means N6 must be able to reach at least N3 or N4), or N2 and N6 become self-elected nodes. In case of the latter, two new main flows propagating in different directions will be generated. The process continues until all 23 nodes have received the message.

IV. Packet formats and protocol for Geo-routing

The routing algorithms described above require information exchange within nodes' neighborhoods, considering link quality, buffer occupancy, and node activity (node turned off or switched on). Furthermore, the total energy and time consumed along the route from the source node to node i, $\bar{E}_i$ and $\bar{\tau}_i$, need to be known. This information is available in the C-hms as well as the data packets as described in detail in the following.

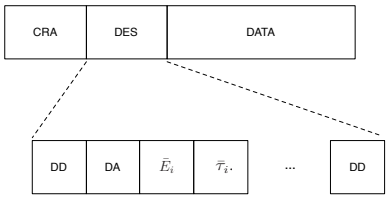

Fig. 3. Data packet structure.

The data packet has a variable length for broadcast and multicast, while its length is fixed for unicast. The packet structure is shown in Figure 3. The three fields are the Current Relay Address (CRA), the DEStination information (DES) and the data contained in the packet (DATA). Within the DES, the DD fields are the destination delimiter consisting of Y_{DD} bits. The DA field reports the Destination Address and it is described by Y_{DA} bits allowing a maximum of $2^{Y_{DA}}$ PLC modems in the network. Furthermore, the fields $\bar{E}_i$ and $\bar{\tau}_i$ indicate the energy and delay spent to reach the current relay, using Y_E and Y_τ bits, respectively. In unicast routing there is a single DA field. In broadcast and multicast, there are multiple DA fields, one for each node still in the set $\mathfrak{U}$. The total length of the DES field for unicast is $(Y_{DA} + 2Y_{DD} + Y_E + Y_\tau)$ bits. In the case of broadcast, we have a total length of $(N-1)Y_{DA} + 2Y_{DD} + Y_E + Y_\tau$ when the packet is sent by the source. Its length is *reduced* along the route, since the number of elements in the set of unreached destinations decreases. In order to give a numerical example, if we have $Y_{DD} = 8$ bits, $Y_E = Y_\tau = 8$ bits and $Y_{DA} = 6$ bits, so as to manage 64 modems, we have a 38-bit DES field for unicast and a maximum length of 170 bits for DES in broadcast. These numbers correspond to a 0.38 ms and 1.7 ms transmission delay a transmission rate of 100 kb/s is considered. Figure 4 illustrates the packet transmission and the shortening of the DES field in a broadcast or multicast transmission along three relay nodes.

The structure of C-hms is shown in Figure 5. The first field is the Neighborhood Delimiter (ND) used to indicate the C-hms start and end. It lasts Y_{ND} bits. The field BS indicates the buffer state of the current relay. It is a number in the set $\{0, 1 \ldots, F\}$, where F is the maximum number of packets

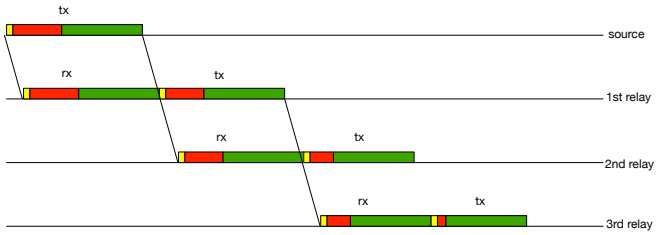

Fig. 4. Illustration of packet transmission and DES field shortening during broadcast or multicast. CRA, DES and DATA fields are in yellow, red and green, respectively.

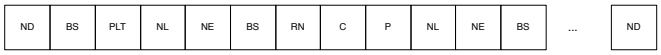

Fig. 5. Cumulative Hello message (C-hms) structure.

that can be stored in the scheduler and represented with $Y_F = \log_2 F$ bits. The field PLT is used by the receiver for channel estimation purposes (and capacity evaluation) and it is characterized by Y_{PLT} bits. The field NL is the Neighborhood Level and indicates if the nodes that are described just after this field are in the same neighborhood ($\mathfrak{N}_i(1)$) of the node transmitting the C-hms or if the nodes are neighbors of neighbors ($\mathfrak{N}_i(2)$) and so forth. The field NE stands for NEighbor and it indicates the label of the node whose parameters, needed for routing, follow in the C-hms and it is characterized by $Y_{NE} = Y_{DA}$ bits. The next BS field is related to NE's buffer state, while the capacity communicated in the C field of Y_C bits, achievable thanks to the use of a P power described by Y_P bits, is evaluated for the link characterized by NE as transmitter and the node RN (represented through $Y_{RN} = Y_{DA}$ bits) as receiver. Then the link/node description continues to include all the nodes in the neighborhood. The last ND field closes the C-hms.

The length of C-hms depends on the neighborhood composition and $K^\star$. Its length can be expressed as $2Y_{ND} + Y_{BS} + Y_{PLT} + \sum_{k=1}^{K^\star} \sum_{\mathfrak{N}_i(k)} (Y_{NL} + Y_{NE} + Y_{BS} + Y_{PLT} + Y_C + Y_P)$. The above summation considers some nodes more than once and this is the price to paid to know the neighborhoods' compositions. As an example, if we assume $Y_{ND} = 8$ bits, $Y_{BS} = 16$ bits, $Y_{PLT} = 4$ bits, $Y_C = 4$ bits and, $Y_P = 4$ bits and each neighborhood composed by four nodes, we have a total length of 1256 bits, that would require 12.56 ms to be transmitted at 100 kbps.

The frequency with which C-hms are sent influences transmission delay and energy for routing. A low signaling rate corresponds to low routing overhead but can lead to outdated node-state and link-state knowledge. A high signaling rate ensures updated neighborhood information at the cost of increased overhead for routing. In relatively dense networks, a strategy that can curb the amount of signaling is to turn off nodes. This would only little affect the network connectivity, since the neighborhoods are still intact.

V. Numerical Results

In this section, we present simulation results for the proposed routing algorithms and compare them with benchmark methods.

A. Simulation Setup

For the simulation experiments, we assume the same PLC transmission parameters as considered in [1], [2] for transmission in the CENELEC A band from 9 kHz to 95 kHz. The test network used in simulations is that depicted in Figure 1. The node-to-node channel transfer functions are obtained from transmission line theory using the Quite Universal Circuit Simulator (QUCS) [26]. We assume NAYY150SE power supply cables and coupling as described in [27, Section 2.3], leading to a per-unit-length (PUL) inductance of 0.33 μH/m and a capacitance of 0.27 nF/m, while PUL conductance and resistance are frequency dependent. To generate different instances of network connectivity, after every 100 sent packets, one uniformly at random selected load impedance is reset according to a uniform distribution between 1 Ω and 9 Ω. Modem impedances of 50 Ω are assumed and replaced by 1000 Ω when a node is switched off. The status of one uniformly at random selected modem is changed after a random time interval uniformly distributed in $[10, 40]$ seconds has elapsed. The parameter $\Gamma = 10$ is used in (5). For simplicity, the noise is assumes as additive white Gaussian noise.

If not specified otherwise, we assume that a second-order neighborhood knowledge is used, where the parameter $Q = 100$ kbps is applied to define a node neighborhood. Furthermore, we use $a_P = 10^3$ J^{-1} and $a_T = 1$ s^{-1} in the cost function (7) so as to tune the delay and energy components to have a comparable order of magnitude, and we choose $\alpha = 2$, $\beta = 2$, $\rho = 0.01$ m^{-1} and $\eta = 2$ in (11)-(13). The packet length for unicast routing is 300 bits, while it varies for broadcast and multicast due to the DES field as described in Section IV. If not specified otherwise, we assume that C-hms are sent every 150 data packets and their length is $24 + 48|\mathfrak{N}_i(1)| + 48|\mathfrak{N}_i(2)|$ bits. The average value we observed is around 400 bits. Finally, unless specified otherwise, the buffer size at each node is 100 packets.

Since the data traffic has an effect on node activity and thus the results, we assume that message generation at nodes follows a Poisson process with mean λ and message size (that is fragmented in packets) is exponentially distributed with mean χ^{-1}, where $\chi = 5$ packets is used thus meaning that each message has an average length of 5 packets. For multiple access we apply Carrier Sensing Multiple Access - Collision Avoidance (CSMA-CA) as often used in PLC systems. This enables nodes to recognize the channel as occupied in case of packet forwarding or signaling due to C-hms. CSMA-CA allows also to manage multiple flows created by self-election. No hidden node problem has been encountered since a node is able to hear the transmission of another node even if this node does not belong to its neighborhood. This is because the neighborhood composition is based on a higher

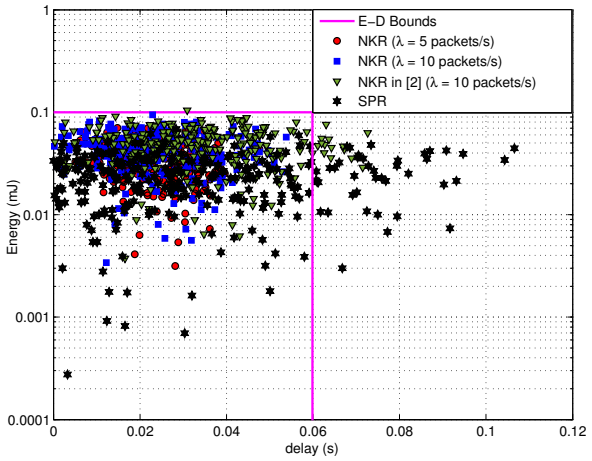

Fig. 6. Energy-delay scatter plot for unicast routing using NKR and SPR when different traffic generation rates are considered.

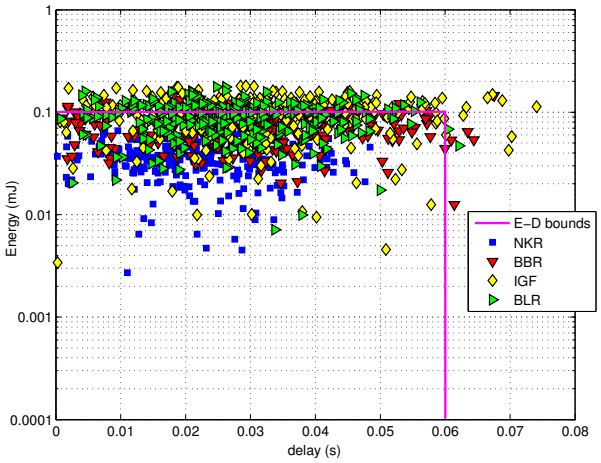

Fig. 7. Energy-delay scatter plot for unicast routing using NKR and BLR, BBR, and IGF for $\lambda = 10$ packets/s.

link quality threshold than that required for the ability of sensing a transmission.

Finally, while the size of node neighborhoods is determined based on the maximum transmitted power, once the next relay is determined, the current node will adapt its power according to $C(P) = Q$, where $C(P)$ is given in (5).

B. Simulation Results

We now present performance results for which we consider delay and energy consumption for routing. For brevity, we refer to the proposed routing as Neighborhood Knowledge-based Routing (NKR).

1) Unicast Geo-routing: Figure 6 shows the energy-delay scatter plot (EDSP) for unicast routing for different levels of traffic, represented by λ. NKR is compared with shortest path routing (SPR) that is a centralized algorithm aiming at minimizing the total energy used for routing without constraints on packet delivery time. The horizontal and vertical lines represent the constraints applied to total energy and delay including that spent for C-hms (which has not explicitly been included in the route optimization). The delay bound of 60 ms is a typical value for several application types[1], see e.g. [28], [29], [30]. The energy bound is set to about six transmissions at full power, following [1].

Each marker in the EDSP represents the energy and delay spent for a source-destination pair obtained as an average over 1000 packets sent considering also network variations. We observe that SPR generally consumes less power than NKR, at the expense of higher delays. In particular, some points for SPR with λ =10 packets/s are outside the area bounded by the constraints. This corresponds to a packet loss as the packet is not delivered within the requested time. NKR meets the constraints, with energy consumption increasing for higher traffic.

[1]We note that the bound used in [2] was smaller as the presence of buffers at the PLC nodes and the statistical traffic generation have not been considered there.

We note that while, for the sake of clarity, the markers in the figure represent an average over 1000 packets, we verified that indeed no packet loss due to violation of the energy or delay bound has occurred for the NKR for the duration of the simulation. The Packet Loss Rate (PLR) for the SPR is 22%.

In Figure 6 we also include the performance of the NKR scheme from [2], for the case of $\lambda = 10$ packets/s. This scheme measures delay in terms of number of hops and uses transmission power instead of energy, so that we adjusted the bounds accordingly. Furthermore, it ignores the traffic level and thus the effect of queuing on delay. It can be seen from the scatter plot that some markers exceed the time threshold, which is due to the less accurate representation of transmission delay in the cost function for selecting the next relay.

In order to evaluate the impact of the different parameters used in the decentralized routing (10), especially those that act directly on the cost function, Table I shows the average required energy E_{ave} and the average delay τ_{ave} per packet (we consider the transmission of 10^6 packets) as well as the PLR for the case of $\lambda = 10$ packets/s and different values for parameters (α, η, β). We recall that α is related to the delay term (11), η to the energy term (12), and β to the distance term (13). Since increasing α means that the difference in delay for two possible relays is amplified, we observe from Table I that it leads to a reduction in delay, but at the price of increasing energy consumption. Similarly, increasing η emphasizes energy consumption over delay. Larger β increases the cost of long links, so it discourages the choice of far relays and thus leads to less energy consumption and a bit higher delays. All these aspects contribute to the PLR. We note that choice of parameters $\alpha = \eta = \beta = 2$ provides a favourable trade-off of the performance indicators for the considered network.

In Figure 7 the proposed NKR algorithm is compared with the above cited BLR [14], IGF [15] and BBR [16]. These methods use knowledge about the immediate neighborhood, i.e., $K^\star = 1$, no constraints on energy consumption and delay, and no power adaptation. IGF applies CSMA/CA with

TABLE I
AVERAGE ENERGY CONSUMPTION, AVERAGE DELAY, AND PLR FOR DIFFERENT PARAMETERS IN (11)-(13).

α	η	β	τ_{ave} (s)	E_{ave} (mJ)	PLR (%)
1.5	1.5	1.5	0.029	0.104	1.5
1.5	1.5	3	0.031	0.098	0.7
1.5	3	1.5	0.033	0.091	0.2
1.5	3	3	0.040	0.084	0.05
2	2	2	0.025	0.085	0.01
3	1.5	1.5	0.026	0.208	0.8
3	1.5	3	0.028	0.174	0.6
3	3	1.5	0.031	0.112	1.0
3	3	3	0.035	0.093	2.1

TABLE II
PACKET LOSS RATE (PLR) AND OVERHEAD FOR BLR, BBR, IGF , NKR

Algorithm	overhead length	overhead energy	PLR
BLR	0%	0%	8%
BBR	2%	60%	11%
IGF	4%	58%	13%
NKR	7%	72%	0.01%

TABLE III
PACKET LOSS RATE (PLR) FOR DIFFERENT TRAFFIC LEVELS AND C-HMS FREQUENCY.

Traffic rate λ	PLR with one C-hms every		
	10 sec	1 sec	0.1 ms
5 packets/s	18%	0.0012%	31%
10 packets/s	35%	0.0043%	42%
15 packets/s	51%	0.0076%	62%

TABLE IV
EFFECT OF TURNING OFF MODEMS ON PACKET LOSS RATE (PLR) FOR DIFFERENT NEIGHBORHOOD DIMENSIONS.

average no. of neighbors in a neighborhood	PLR
2	17%
4	1.84 %
5	0.009%
6	0.0022 %

RTS-CTS signaling. We observe from Figure 7 that BLR is often less energy-efficient than NKR even though it does not require signaling. This is due to packet duplication in BLR as discussed in [1]. While IGF avoids packet duplication, it requires RTS-CTS signaling, leading to somewhat higher delays compared to BLR. BBR uses hello-messages that are not as costly as RTS-CTS to avoid packet duplication. The proposed NKR provides a better performance trade-off than also BBR, even though a proper setting of signaling (C-hms) must be carried out.

Table II shows the PLR (evaluated on the basis of 10^6 packets sent) and signaling overhead for the different schemes. We report two different measures of overhead. The "overhead length" and represents the length of signaling messages with respect to the total length of signaling and data messages. The second measure is "overhead energy", which reports the relative amount of energy used for signaling with respect to the total energy consumed for transmission. It thus factors in the different frequencies of messages. While BLR does not need signaling, IGF uses signaling for each packet to forward and both current relay and next relay exchange messages. The overhead for BBR and NKR depends on the frequency of sending hello messages, which reflects in different PLRs. The performance gain in terms of PLR exhibited by NKR can further be explained by noting that it applies power allocation, while the other methods transmit at full power, and, besides, NKR has more knowledge about the subsequent routing steps, while the other algorithms are limited to only one neighborhood.

In this context, an interesting comparison is to benchmark NKR with an idealized centralized routing scheme that has instantaneous and perfect network status knowledge, i.e., the solution of (8) without accounting for signaling overhead. This idealized scheme leads to an average delay of 0.022 s and energy of 0.008 mJ, with a PLR of 0.008% compared to 0.025 s and 0.085 mJ for NKR, respectively. The latter energy figure divides into 0.019 mJ for routing a packet, while the remaining 0.056 mJ are due to signalling via C-hms (and thus varies with the C-hms signaling interval). Hence, we observe that the delay and energy-for-routing performance of NKR is quite competitive to what is achieved with centralized routing as well as the PLR. With regard to signaling overhead, we note that the average energy consumption for BBR and IGF are 0.120 mJ and 0.140 mJ, respectively, of which 0.072 mJ (BBR) and 0.082 mJ (IGF) are used for signaling. Or in other words, as shown in Table II, BBR and IGF spent 60% and 58% of the energy for signaling, respectively, which is quite comparable to the 72% in the NKR scheme (which overall achieves a better energy-delay performance). Clearly, the signaling overhead for a centralized scheme would be considerably larger.

The role of C-hms transmissions is emphasized in Table III, which shows the PLR as a function of the frequency of C-hms signaling and traffic rate. Despite of the previous results, where we transmitted few packets for each node/destination, here we still consider 10^6 packets in order to measure low PLR. So the results shown in Figs. 6 and 7 are able to capture the main characteristics of the behavior of algorithms. In fact, for average performance outside the bounds, it is expected that several packets sent do not meet the constraints. The C-hms values reported in Table III refer to the time that passes between two C-hms sent by two nodes in the network. We observe that infrequent update of channel information leads to outdated neighborhood knowledge. On the other hand, sending C-hms very frequently can overload the network with side information. Hence, a compromise should be obtained between being updated about network and overhead for acquiring such information. Furthermore, even though in Table III, a frequency of one C-hms every second provides a good trade-off for different traffic levels, that value could not be the best choice if we consider different network topologies. Finding the optimal value for C-hms frequency is an worthwhile task beyond the scope of this contribution.

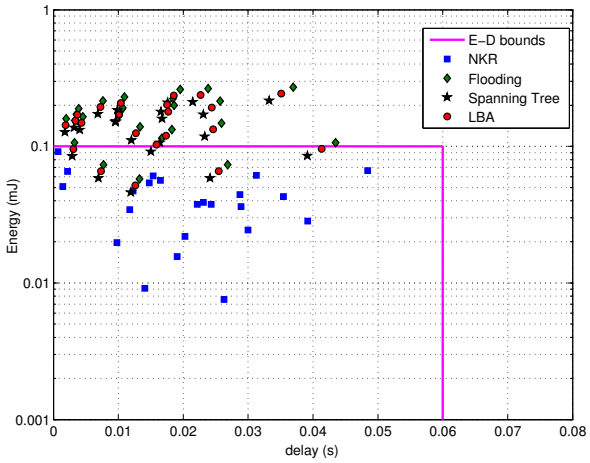

Fig. 8. Energy-delay scatter plot for broadcast routing.

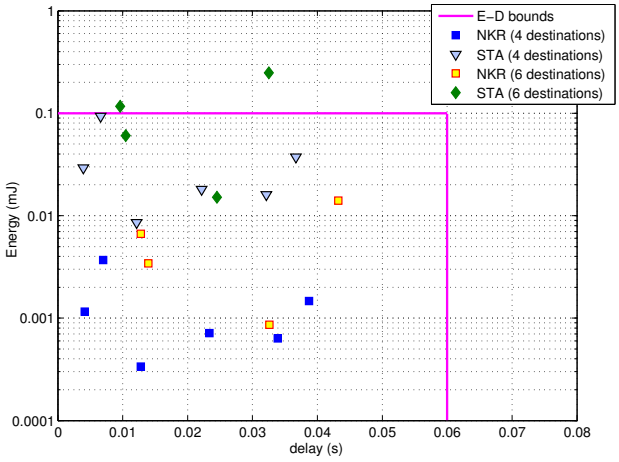

Fig. 9. Energy-delay scatter plot for multicast routing.

Table IV shows the effect of turning off modems if they are neither a source nor a selected relay for at least one message for 120 seconds. This duration was chosen as it is a sufficiently long time for a node to determine that despite changes in source-destination combinations and neighborhood compositions, it is largely redundant from a routing point of view. For this purpose, what we experienced is that usually this reflects in turning off nodes N3, N7, N12, N14, N21 and N23 not necessarily at the same time, even multiple of those sometimes are turned off. Table IV presents the PLRs for different values of the average number of neighbors in a neighborhood, which has been adjusted through selecting, for each simulation, a different Q value. For example, $Q = 500$ kbps leads to an average of two neighbors per neighborhood, while $Q = 75$ kbps results in an average of six neighbors per neighborhood. Considering that the PLR ranges from 0.0022% to 17%, sleep modes for nodes to save power are suitable in sufficiently populated neighborhoods (corresponding to low rate transmission), while nodes should remain active if the neighborhood population is low (in the case of high rate transmission).

2) Broadcast Geo-routing: Figure 8 shows the EDSP related to the total energy and maximum delay spent for achieving all the nodes within power and delay constraints of 10^{-4} Joule and 60 ms, respectively, for $Q = 200$ kbps. We consider the proposed NKR scheme as well as flooding, spanning tree routing [31] and LBA [18] and we transmit 1000 packets for each source node. Flooding is implemented such that each node forwards a packet only once. We observe that the performances of flooding, spanning tree and LBA routing are very similar since they transmit at full power and focus on delay minimization. Moreover, spanning tree uses flooding to establish paths. The proposed NKR assures relatively lower energy consumption. The maximum delay is somewhat higher than for the other methods, but the delay bound is met and no packet loss is experienced. The PLR for flooding, spanning tree and LBA are 65%, 53% and 57%, respectively. It is important to highlight that PLR can increase if the number of packets transmitted increases (so as to have the ability of measuring very low PLR) or if the bounds would change and become more strict.

3) Multicast Geo-routing: Figure 9 shows the EDSP when multicast routing is operated. We consider node N1 as source and randomly select destinations. Moreover, the parameters are the same used for the broadcast case. We consider what happens when we select six different groups each containing four destinations ($|\mathcal{D}| = 4$) and four different groups each one having six destinations ($|\mathcal{D}| = 6$). Then we simulate the transmission of 1000 packets and each marker in the EDSP represents the maximum delay and the total energy spent for delivery the packet to all the destinations belonging to the above mentioned randomly selected sets. We compare NKR with multicast routing using the Steiner Tree Algorithm (STA) as in [25]. We observe comparable or somewhat lower delays for the STA solution. Since it however does not include an energy optimization or constraint, NKR achieves a better performance in this metric. The NKR algorithm allows to deliver packets within requested time and energy constraints, so no packet losses are experienced. The PLR for STA presents is 2% for 4 destinations and 9% for 6 destinations.

VI. Conclusion

In this paper, we have presented routing algorithms and protocols that use static information about the network topology and updated local information about network performance parameters to efficiently pass messages in a PLC network. The proposed algorithms solve the routing problem under energy and delay constraints, so as to meet requirements from smart grid applications on message delivery time and to avoid undue energy consumption for the communication task. For the simulated example of a smart grid communication network, they outperform solutions already available in the literature without increasing the complexity of the system.

References

[1] M. Biagi and L. Lampe, "Location assisted routing techniques for power line communications in smart grids," in *IEEE International Conference*

on Smart Grid Communiations (SmartGridComm), Gaithersburg, USA, Oct. 2010.

[2] M. Biagi, S. Greco, and L. Lampe, "Neighborhood-knowledge based geo-routing in PLC," in *IEEE Intl. Symp. Power Line Commun. (ISPLC)*, Mar. 2012, pp. 7–12.

[3] P. Brown, "Power line communcations - Past, present and future," in *Intl. Symp. Power Line Commun. (ISPLC)*, Lancaster, UK, Mar./Apr. 1999.

[4] D. Dzung, I. Berganza, and A. Sendin, "Evolution of powerline communications for smart distribution: From ripple control to OFDM," in *IEEE Intl. Symp. Power Line Commun. (ISPLC)*, Apr. 2011, pp. 474–478.

[5] S. Galli, A. Scaglione, and Z. Wang, "For the grid and through the grid: The role of power line communications in the smart grid," *Proc. IEEE*, vol. 99, no. 6, pp. 998–2017, 2011.

[6] H. Li and W. Zhang, "Qos routing in smart grid," in *Global Telecommunications Conference (GLOBECOM 2010), 2010 IEEE*, Dec 2010, pp. 1–6.

[7] N. Saputro, K. Akkaya, and S. Uludag, "A survey of routing protocols for smart grid communications," *Computer Networks*, vol. 56, no. 11, pp. 2742 – 2771, 2012. [Online]. Available: http://www.sciencedirect.com/science/article/pii/S1389128612001429

[8] A. Sabbah, A. El-Mougy, and M. Ibnkahla, "A survey of networking challenges and routing protocols in smart grids," *Industrial Informatics, IEEE Transactions on*, vol. 10, no. 1, pp. 210–221, Feb 2014.

[9] K. Razazian, A. Niktash, V. Loginov, J. LeClare, T. Lys, and C. Lavenu, "Experimental and field trial results of enhanced routing based on LOAD for G3-PLC," in *IEEE Intl. Symp. Power Line Commun. (ISPLC)*, Mar. 2013, pp. 149–154.

[10] M. Vucinic, B. Tourancheau, and A. Duda, "Performance comparison of the RPL and LOADng routing protocols in a home automation scenario," in *IEEE Wireless Communications and Networking Conference (WCNC)*, Apr. 2013, pp. 1974–1979.

[11] O. Balmau, D. Dzung, A. Karaagac, V. Nesovic, A. Paunovic, Y. Pignolet, and N. Tehrani, "Evaluation of RPL for medium voltage power line communication," in *IEEE International Conference on Smart Grid Communications (SmartGridComm)*, Nov. 2014, pp. 446–451.

[12] G. Bumiller, L. Lampe, and H. Hrasnica, " Power Line Communications for Large-Scale Control and Automation Systems," *IEEE Commun. Mag.*, vol. 48, no. 4, pp. 106–113, Apr. 2010.

[13] J. Sanchez, P. Ruiz, and R. Marin-Perez, "Beacon-less geographic routing made partical: Challenges, design guidelines and protocols," *IEEE Commun. Mag.*, vol. 47, no. 8, pp. 85–91, Aug. 2009.

[14] M. Heissenbüttel, T. Braun, T. Bernoulli, and M. Wälchli, "BLR: Beacon-Less Routing Algorithm for Mobile Ad-Hoc Networks," *Elsevier J. Comp. Commun.*, vol. 27, no. 11, pp. 1076–1086, Jul. 2004.

[15] B. M. Blum, T. He, S. Son, and J. A. Stankovic, "IGF: A State-Free Robust Communication Protocol for Wireless Sensor Networks," CS Department, University of Virginia, Tech. Rep., 2003.

[16] L. Demoracski, "Fault-tolerant beacon vector routing for mobile ad hoc networks," in *19th IEEE Intern. Parallel and Distributed Processing Symposium (IPDPDS)*, 2005.

[17] S.-G. Yoon, S. Jang, Y.-H. Kim, and S. Bahk, "Opportunistic routing for smart grid with power line communication access networks," *IEEE Trans. Smart Grid*, vol. 5, no. 1, pp. 303–311, Jan. 2014.

[18] M. Khabbazian, I. Blake, and V. Bhargava, "Local broadcast algorithms in wireless ad hoc networks: Reducing the number of transmissions," *Mobile Computing, IEEE Transactions on*, vol. 11, no. 3, pp. 402–413, March 2012.

[19] D. Borsetti and J. Gozalvez, "Infrastructure-assisted geo-routing for cooperative vehicular networks," in *Vehicular Networking Conference (VNC), 2010 IEEE*, Dec 2010, pp. 255–262.

[20] D. Goldin, M. Song, A. Kutlu, H. Gao, and H. Dave, "Georouting and delta-gathering: Efficient data propagation techniques for geosensor networks," in *First Workshop on Geo Sensor Networks*, 2003, pp. 9–11.

[21] D. Koutsonikolas, S. Das, H. Charlie, and I. Stojmenovic, "Hierarchical geographic multicast routing for wireless sensor networks," in *Sensor Technologies and Applications, 2007. SensorComm 2007. International Conference on*, Oct 2007, pp. 47–354.

[22] J. Sanchez, P. Ruiz, J. Liu, and I. Stojmenovic, "Bandwidth-efficient geographic multicast routing protocol for wireless sensor networks," *Sensors Journal, IEEE*, vol. 7, no. 5, pp. 627–636, May 2007.

[23] K. Zhu, B. Zhou, X. Fu, and M. Gerla, "Geo-assisted multicast interdomain routing (GMIDR) protocol for MANETs," in *Communications (ICC), 2011 IEEE International Conference on*, June 2011, pp. 1–5.

[24] D. Kim, S. Song, and B.-Y. Choi, "Energy-efficient adaptive geosource multicast routing for wireless sensor networks," *Sensors Journal, Hindawi*, February 2013.

[25] N. Skorin-Kapov and M. Kos, "The application of steiner trees to delay constrained multicast routing: a tabu search approach," in *International Conference on Telecommunications (ConTEL)*, vol. 2, Jun. 2003, pp. 443–448 vol.2.

[26] Q. Team, *Quasi Universal Circuit Simulator*, 2015. [Online]. Available: http://http://qucs.sourceforge.net

[27] H. Ferreira, L. Lampe, J. Newbury, and T.G. Swart (Editors), *Power Line Communications*. John Wiley & Sons, 2010.

[28] C. Nguyen and A. Flueck, "Modeling of communication latency in smart grid," in *IEEE Power and Energy Society General Meeting*, Jul. 2011, pp. 1–7.

[29] P. Kansal and A. Bose, "Bandwidth and latency requirements for smart transmission grid applications," *IEEE Trans. Smart Grid*, vol. 3, no. 3, pp. 1344–1352, Sep. 2012.

[30] F. Aalamifar, L. Lampe, S. Bavarian, and E. Crozier, "WiMAX technology in smart distribution networks: Architecture, modeling, and applications," in *IEEE PES TD Conference and Exposition*, Apr. 2014, pp. 1–5.

[31] "IEEE Draft Amendment 3 to 802.1Q Virtual Bridged Local Area Networks: Multiple Spanning Trees - IEEE Draft Amendment to IEEE Std 802.1Q-1999 (Superseded by 802.1S-2002) (Incorporated Into 802.1Q-2003)," *IEEE Std P802.1s/D14.1*, pp. –, 2002.